Hyperfine Interact (2019) 240: 44
https://doi.org/10.1007/s10751-019-1577-8

Magnetite and the Verwey transition, from γ-rays to low-energy electrons

Juan de la Figuera[1] · **José F. Marco**[1]

Published online: 6 May 2019

Abstract
Magnetite, a semiconducting ferrimagnetic iron spinel with a metal-insulator phase transition, the Verwey transition, has long been the subject of Mössbauer spectroscopy studies, which continue today. We review the current status of the understanding of the Mössbauer spectra of magnetite. Furthermore, magnetite is a very attractive material in current topics such as spintronics. In this particular subject, to determine the behavior of magnetic domains is paramount, and the changes ocurring on the near surface region upon undergoing the Verwey transition are relevant. In order to advance in this area, we have incorporated some new techniques, namely microscopy observations made with low-energy electrons. These observations can be performed upon changing the temperature, and can provide magnetic contrast through the use of spin-polarized electrons. By this means, we have observed the ferroelastic transformation associated with the Verwey transition, discovered an order-disorder transition of the (001) surface of magnetite and observed the changes in the magnetic domains on the same surface by changing the temperature. Low-energy electrons also are the key to the Mössbauer experiments of magnetite films and surfaces, with the promise of providing surface-sensitive spatially resolved Mössbauer spectra.

Keywords Magnetite · Surfaces · Magnetism · Low-energy electrons · Low-energy electron microscopy · Mössbauer spectroscopy · Verwey transition

PACS 75.50.Gg · 76.80.+y · 75.70.i · 71.30.+h

This article is part of the Topical Collection on *Proceedings of the 16th Latin American Conference on the Applications of the Mössbauer Effect (LACAME 2018), 18–23 November 2018, Santiago de Chile, Chile*
Edited by Carmen Pizarro Arriagada

✉ Juan de la Figuera
juan.delafiguera@csic.es

José F. Marco
jfmarco@iqfr.csic.es

[1] Instituto de Química Física "Rocasolano", Madrid E-28006, Spain

1 Introduction

Magnetite is the first magnetic material to appear in the history of mankind [1], having been used both by Chinese and Greeks thousands of years ago. It has also been a constant source of interest during the development of modern condensed matter physics, spanning from the first steps in the use of x-ray diffraction to determine atomic structures [2] to the subject of metal insulator transitions. Magnetite [3] is a conducting mixed-valence iron oxide which crystallizes in the inverse spinel structure at room temperature. Thus, the spinel octahedral sites are occupied by Fe^{3+} and Fe^{2+} while the tetrahedral sites are only populated by Fe^{3+}. Due to electron hopping between the octahedral Fe^{3+} and Fe^{2+} cations, magnetite is a conductor. Both octahedral and tetrahedral cations are ferromagnetically coupled within each site, while the coupling is antiferromagnetic between the two sites. At room temperature, all the tetrahedral sites are equivalent, as well as all the octahedral ones. Magnetite has the largest saturation magnetization of any iron oxide, of 4.06 μ_B per Fe_3O_4 formula unit, or 1.35 μ_B per Fe cation. Together with the high Curie temperature (858 K) this explains its use in magnet applications. However it is a rather soft magnet with a low magnetocrystalline anisotropy at room temperature [4]. Its magnetocrystalline anisotropy, furthermore, changes substantially with temperature, and in a non-monotonic way [5]. At room temperature it favors the $\langle 111 \rangle$ as easy axes, although upon cooling down the easy axes switch to the $\langle 100 \rangle$ ones at the so-called isotropic point (around 140 K).

When cooling down through 122 K for pure samples, the so-called Verwey temperature, magnetite undergoes a metal-insulator transition, where the resistivity increases by two orders of magnitude [6]. This transition has been the subject of a multidecade discussion concerning its origin and particular details, discussion that continues today [7, 8]. A particular area of disagreement has been the particular charge order (if any!) observed in the low-temperature phase. An accurate model of the low-temperature phase of magnetite is crucial to understand the Verwey transition because it defines the ground state of the structure. But while the room temperature structure was determined to be a cubic inverse spinel at the dawn of x-ray diffraction analysis [2], the low-temperature phase has been more difficult to solve. Soon after the discovery of the Verwey phase transition, it was attributed to a freezing of the electron hopping along the rows of octahedral iron cations: below the transition such freezing was suggested to give rise to alternating Fe^{3+} and Fe^{2+} rows, so a doubling of the unit cell was expected at low temperatures. However, such low temperature cell size was soon proved to be incorrect. This initiated the search for the charge ordering of the low temperature phase. Magnetite has some properties that have complicated the determination of the structure of the low temperature phase. On one hand, the Verwey transition is quite dependant of the crystal quality and specific composition of a given sample. The magnetite spinel structure can accept a rather large range of non-stoichiometries, which often are difficult to measure accurately and can have a strong impact on the details of the Verwey transition. In fact, the transition is only first order for compositions which are close to the stoichiometric one, becoming second order otherwise [4]. On the other hand, that the low temperature structure has the Cc symmetry implies that it has 24 different domains that can, and do, appear in a crystal cooled through the Verwey transition. Such twinning often occurs at the micron scale [9, 10]. Only in the beginning of the second decade of the XXI century a widely accepted detailed atomistic model was proposed [11] and deemed accurate enough to use as the starting point for understanding the magnetite structure. This model was based on x-ray diffraction acquired on a twin-free 40 μm crystal. The current description of the low temperature phase [11] has 16 inequivalent octahedral positions and 8 inequivalent tetrahedral ones. The charge order is based on a network of corner sharing

"trimeron" units. Each "trimeron" is a linear arrangement of three octahedral cations: two Fe^{3+} ones around a Fe^{2+} one at the center.

Although the current low-temperature model of magnetite has represented a substantial advance to understand magnetite and its metal insulator transition, the role of the surface is still complicating the situation. This is particularly true as many of the techniques used to study the magnetic properties of magnetite can be strongly surface-dependent. Then the traditional problems presented on bulk magnetite, are compounded by the need to understand the near surface region, often with atomic precision [12]. For example, the (001) surface of magnetite can nowadays be prepared in such a manner that a reproducible surface is obtained, using sputtering and annealing cycles. However, at room temperature such surface is reconstructed relative to the bulk truncated one. The surface reconstruction has a $\sqrt{2} \times \sqrt{2}R45°$ periodicity [12]. It has been proposed as a low-temperature surface counterpart to the bulk below-Verwey state [13]. As this reconstruction is stable at room temperature, that surface Verwey proposal was very exciting for the community. We will show that an accurate structural determination of the near surface region was required to disprove any possible surface Verwey transition linked to the surface structure [14].

2 Mössbauer observations on bulk magnetite

Mössbauer spectroscopy was applied to magnetite quite early in the history of the recoiless nuclear resonant absorption. The first publications are from 1961 [15], barely a couple of years later after the Mössbauer effect discovery. Maybe it is more surprising that when this publication was being written, over 2000 publications on the subject of the Mössbauer technique applied to magnetite have been published.

The spectrum at room temperature is rather simple, and it consists of two easily resolved Zeeman sextets. The two components overlap slighly. The area ratio of the two components is 1:2 within the experimental error. It is straightforward to assign each component to Fe cations in the tetrahedral and the octahedral sites respectively. In particular the first one has a typical isomer shift of 0.27 mm/s and negligible quadrupole shift, characteristic of tetrahedrally coordinated Fe^{3+}. The hyperfine field is close to 49 T. The second component, with twice the area, has an isomer shift of 0.67 mm/s, intermediate for octahedral Fe^{2+} and Fe^{3+}, and again a neglible quadrupole shift, together with an hyperfine field of 46 T. These parameters are in reasonable agreement with identifying the second sextet as corresponding to $Fe^{2.5+}$ in octahedral environment. The oxidation state arises from electron hopping between octahedral Fe^{2+} and Fe^{3+} during the Mössbauer observation time, which is of the order of 10^{-8} s. This component has a larger linewidth that the tetrahedral iron one. Häggström et al. [16] showed that the origin of this increase in linewidth is compatible with two distinct but related effects. On one hand, considering the magnetic dipolar interaction of the neighbors around each octahedral cation, there are two families of inequivalent magnetic cations within a single magnetic domain, present with a population in the ratio 3:1. This gives rise to two components with slightly different local magnetic fields. On the other hand, those two families of cations should also present shifted Mössbauer resonance lines related to the angle between the local magnetic field and the main component of the electric field gradient. Again that amount is different for the two types of octahedral cations in each magnetic domain. Note that this implies that the second contribution is related to the particular easy axes of the sample. A recent Mössbauer spectra reported [17], using the mentioned fit to three components, is shown in Fig. 1a.

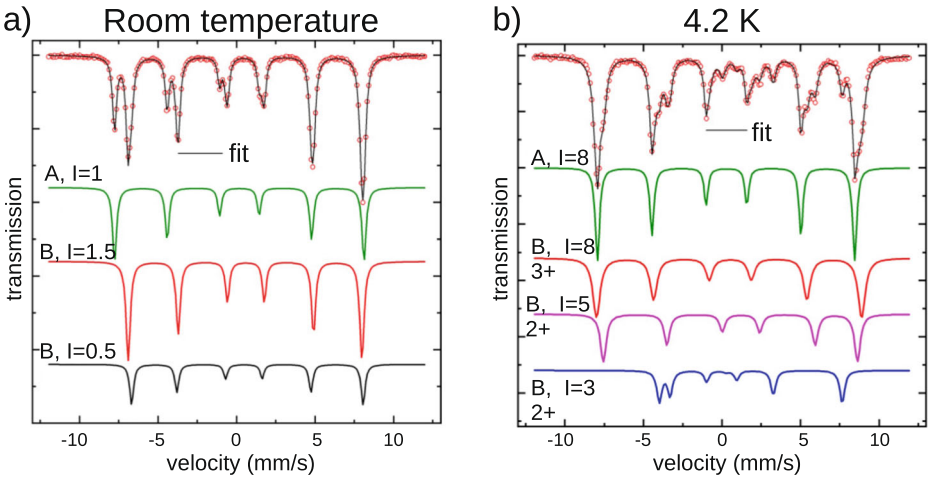

Fig. 1 **a**, **b** Mössbauer spectra from a magnetite single crystal at room temperature and below the Verwey temperature, respectively. Adapted with permission from Ref. [17]

The below-Verwey Mössbauer spectra has also been measured repeteadly [15, 18, 19]. However, the spectrum is much more complex that the room temperature one, as shown in Fig. 1b. And a variety of fit components have been used in the past. As reported by Ref. [18], fits have been published to either three, four, five [19], six or even nine sextets. In each case, the fit was suggested by phenomenological arguments, to justify the introduction of components corresponding to particular Fe^{3+} or Fe^{2+} cations in different sites. However, the fits themselves could not be used to prove one or other right, as the significant overlap between components made the fits comparable in quality. In retrospect, this is to be expected as the present model of the low-temperature phase of magnetite [11] considers 24 inequivalent cation positions. Using the current model as starting point, Řezníček et al. [20] have reinterpreted the low-temperature Mössbauer spectra of magnetite. As a first step and for the trimeron structure they calculated the expected isomer shift, quadrupole shift and hyperfine fields of each of the inequivalent iron cations by density functional theory [20, 21]. Then they proceeded to group the iron cations by similar Mössbauer parameters. In this way, they suggest that a fit to four different components is a reasonable compromise to reproduce the experimental data. They thus proposed a decomposition of the experimental spectrum into $8\times Fe^{3+}$ in tetrahedral sites, and $8\times$ octahedral Fe^{3+}-like sites, $5\times$ octahedral Fe^{2+}-like sites and finally another set of $3\times$ octahedral Fe^{2+}-like sites. Such fit is shown in Figure 1b. Note that as the authors remark, to identify the individual iron sites in the experimental spectra is "futile" [20]. On an historical note, the ratio of the proposed Fe^{2+}-like sites is not to different for a similar four component decomposition proposed decades ago [22]. However, now there is a firm footing to justify such a fit.

3 Observations with low-energy electrons of the (001) surface of magnetite

As mentioned before, the (001) surface of magnetite, while it is not the lowest energy surface (that being the (111) surface) is however one of its most studied compact surfaces [12,

23]. One reason is that repeated cycles of sputtering and annealing in ultra-high vacuum produce a reproducible surface that can thus be characterized in detail in different laboratories. However, such surface has a different periodicity than the bulk-truncated surface. Its low-energy electron diffraction pattern corresponds to a $\sqrt{2}\times\sqrt{2}$R45° pattern relative to the surface (bulk) truncated one. This surface is terminated in oxygen anions attached to octahedral iron cations. The octahedral iron cations form rows along ⟨011⟩ in-plane directions and are visible in scanning tunneling microscope (STM) images [12], showing a characteristic undulating pattern of the iron cations rows that gives rise to the $\sqrt{2}\times\sqrt{2}$R45° pattern.

Given the context of the described Mössbauer experiments on bulk magnetite, one crucial question is what changes, if any, the surface undergoes when going through the bulk Verwey transition. And, conversely, which changes can be ascribed uniquely to the surface. In particular it is of interest whether there are any phase transitions that the surface undergoes with temperature. In order to answer these questions, we resort to experiments performed by imaging reflected low-energy electrons.

Low-energy electrons are well suited to explore surfaces thanks to the strong interaction with the last layers of a material. They have been used in the so-called low-energy electron microscopes (LEEM) [24, 25]: microscopes that use regular electronic lenses to image the distribution of electrones reflected from a surface at low energies. These instruments were introduced a couple of decades ago by E. Bauer and are now available at several laboratories in the world. They provide a nanometer-resolution real-space view of surfaces in ultra-high vacuum employing electrons in the energy range of a few eV to tens of eV. Additionally, the instruments provide low-energy diffraction patterns of selected areas of the surface [26].

A typical image of the (001) surface of a magnetite crystal is shown in Fig. 2a. The image shows square like protrusions and faint lines which correspond to step bunches on the surface of the crystal. The crystal has been cleaned by the standard procedure of repeated sputtering with Ar^+ ions at typical energies of 1000 eV followed by annealing to 800 K in oxygen to reorder the surface after the sputtering step. Upon cooling through the Verwey transition [10], an array of parallel lines appear on the surface (see top row of Fig. 2a-c). The rows of parallel lines are shown to consist of alternating bright and dark bands (see Fig. 2d), with a typical width of 500 nm. They are unperturbed by surface features. The bands correspond to microtwins, with a shallow inclination angle of 0.23° relative to the surface plane. The bright/dark contrast is due to the misalignment of the surface relative to the illuminating electron beam [10]. The observed structure corresponds to the microtwinning reported by transmission electron microscopy [9] and expected on the monoclinic sub-Verwey magnetite crystal. The twins are connected through their a-b monoclinic sides. A direct observation by scanning tunnelling microscopy [10] confirmed the inclination of the surface, which forms a "roof"-like structure. However, at the atomic scale there was no change observed whatsoever on the reconstructed surface: the same atomic arrangement was observed above and below the Verwey transition [10]. Thus, no structural modification on the surface, other than the appearance of twins which is a bulk effect due to the change from the cubic to the monoclinic structure, has been detected so far.

So we are left to consider the surface reconstruction itself. This is another example where the knowledge of the structure is crucial to understand the underlying physics. It is thus of historical interest to follow the understanding of this surface. The surface has been predicted to be insulating, in contrast with bulk magnetite. A particular striking model for the surface [13, 27] suggested an electronic origin for the undulations of the Fe cations that are characteristic of the reconstruction, associated with the emergence of charge order in the subsurface. It was further supported by density functional theory calculations combined with low-energy electron diffraction multiple scattering calculations reproducing

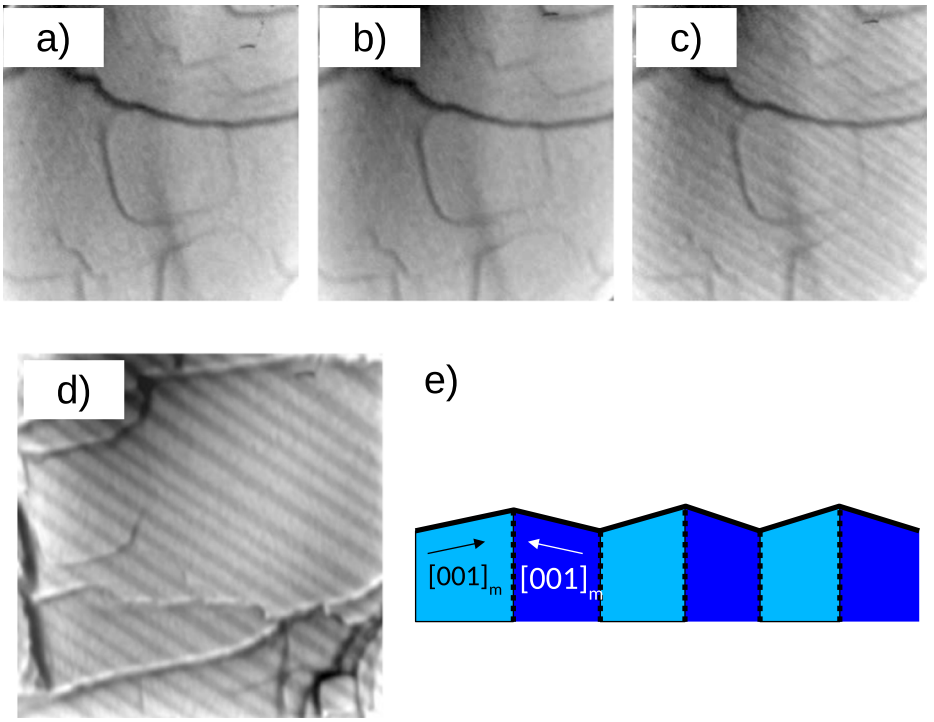

Fig. 2 **a**–**c** LEEM images of a magnetite (001) surface from a movie acquired upon cooling through the Verwey transition. Frame **b** is above the Verwey transition, while frame **c** is below. The images are 8.6 μm wide. **d** Higher resolution image of the magnetite surface below the Verwey transition. **e** Schematic of the twin structure that gives rise to the bands observed in **c**) and **d**). Adapted from Ref. [10]

experimental electron [28] and surface x-ray diffraction [27] data. The origin of the reconstruction was suggested to be a Jahn-Teller-like distortion [27] along the octahedral iron cations that would minimize the total energy. Such origin would make the surface reconstruction an analog of the below-Verwey bulk phase. If such were the case then increasing the temperature of the surface, a phase transition should eventually be observed.

By means of LEEM the diffraction pattern can easily be followed at different substrate temperatures. As shown in Fig. 3, there is actually a phase transition on the surface, at 454°C as described in detail in Ref. [29]. While at lower temperature the pattern presents the $\sqrt{2} \times \sqrt{2}$R45° reconstruction, at high temperature the surface shows a simpler pattern which reflects the bulk truncated structure periodicity. In order to characterize the surface phase transition, the evolution of one of the reconstruction diffracted beams (marked with a circle in Fig. 3a) intensity with temperature is shown in the lower panel of the same figure. In the plot, a fit to a two dimensional Ising model is plotted also. It is clear that below the transition temperature, the evolution of the diffracted beam closely resembles the fit. This implies that the surface undergoes an order-disorder transition which is a second order one.

A final piece of the puzzle was reported in 2014 [14]. In an extensive low-energy diffraction intensity-vs-energy study of the reconstruction, Parkinson et al. determined that the structure of the surface actually corresponds, not to a Jahn-Teller distortion of the octahedral rows, but rather to literally a surface reconstruction: two sub-surface tetrahedral iron cations are missing, and an extra tetrahedral cation is located at a sub-surface position not

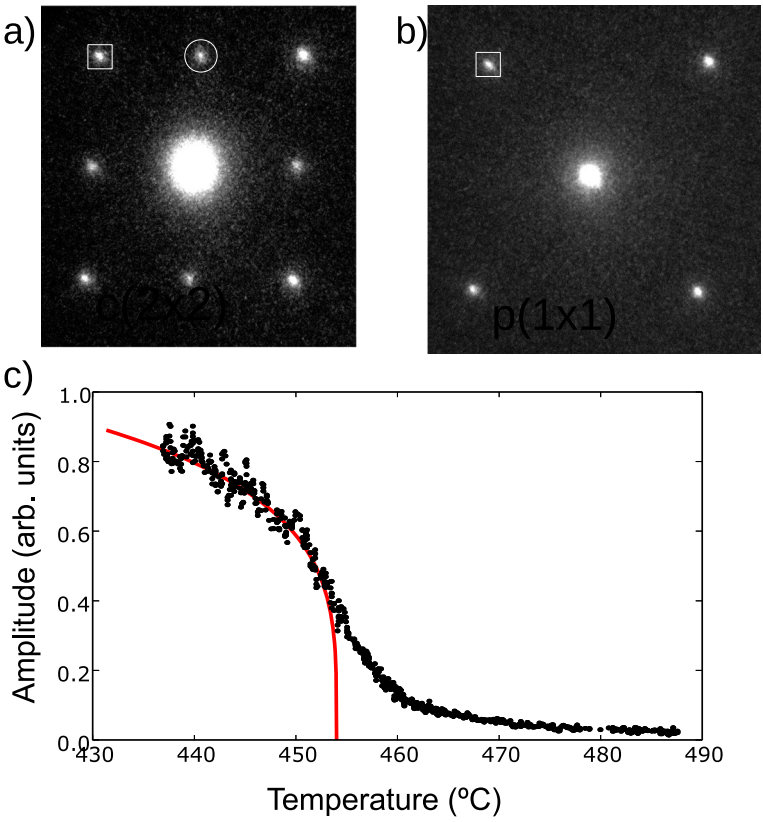

Fig. 3 **a** LEED pattern of the reconstructed surface of magnetite (001) acquired in a LEEM. **b** LEED pattern at high temperature showing the LEED pattern whose periodicity corresponds to the truncated bulk termination. **c** Intensity of the diffracted beam marked with a circle in **a**) vs temperature. Adapted from Ref. [29]

filled in the bulk. This arrangement of iron cations in the near surface region produce the observed distortions identified by STM. This accurate model of the reconstructed surface also explained other experimental observations difficult to reconcile with the electronic origin of the reconstruction, such as the stability of Au atoms on the reconstructed surface [30]. The observed surface order-disorder transition [29] then corresponds to a disordering of such arrangement. It has no relation whatsoever with any type of surface Verwey transition.

Thus, in summary, no local effect on the surface has been detected either through the bulk Verwey transition [10] nor through the recently discovered surface phase transition of magnetite [29]. It remains to be determined whether the surface affects the Verwey transition in any other way.

4 Observations with spin-polarized electrons on the (001) surface of magnetite

Magnetic properties are strongly affected by the Verwey transition in magnetite [5]: the magnetocrystalline anisotropy changes substantially, new easy axes appear, and the

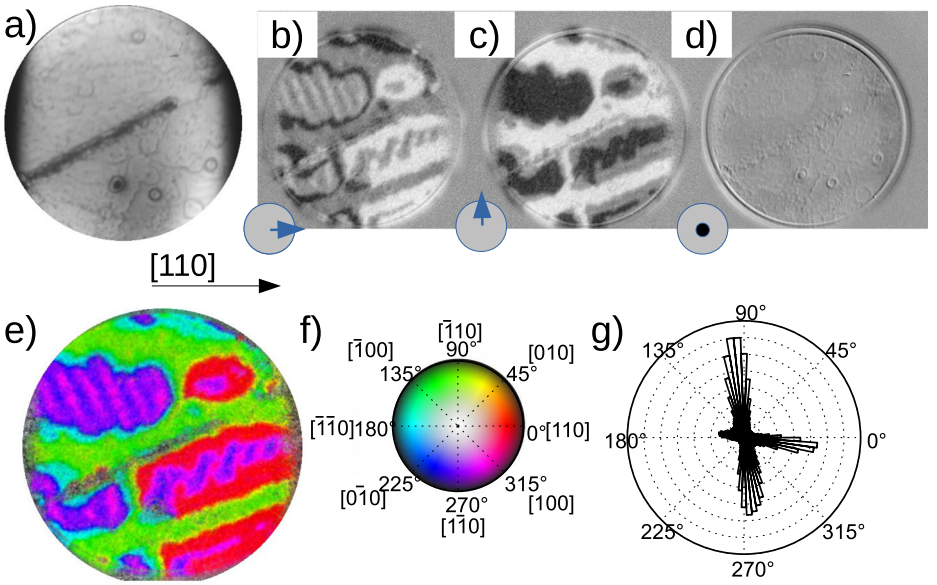

Fig. 4 **a** LEEM image, with a field of view of 12 μm. **b**, **c**, **d** SPLEEM images showing the magnetic contrast in the same area along the x-axis of the figure, the y-axis and perpendicular to the surface respectively. The images have been acquired at room temperature. **e** Color image showing the angle of the magnetization with the colormap shown in **f**). **g** Histogram of the magnetization angles, from the image shown in **e**)

distribution of magnetic domains changes drastically [9]. While TEM has been used to observe the magnetic domains through the Verwey transition [9, 31], most of the nanometer scale observations on the (001) surface have been done by means of spin-polarized low-energy electron microscopy (SPLEEM, [24, 25, 32]). In SPLEEM, a spin-polarized beam of electrons is used in a LEEM instrument as the illumination source. The spin-dependent reflectivity is measured by performing a pixel-by-pixel substration of images acquired with opposite spin-polarization. This provides a magnetic contrast image in ferro or ferrimagnetic materials, where white areas indicate a magnetization along the first image spin-polarization direction, black areas indicate that the magnetization points in the opposite direction, while grey areas mark regions where either there is no magnetization, or the magnetization is perpendicular to the electron-beam spin direction. Such a SPLEEM image is shown in Fig. 4b corresponding to an spin-direction of the incoming electron beam along the x-axis of the figure. By means of a spin-manipulator [33], the spin direction can be oriented along any sample direction. In Fig. 4b–d three orthogonal components of the surface magnetization are measured in turn. Then the magnetization vector can be reconstructed pixel-by-pixel by combining the known three components. The results is represented in Fig. 4e, where a color palette (f) is used to indicate the in-plane angle of the magnetization. Another way to summarize the information is to plot an histogram of the magnetization orientations through the image. As shown in Fig. 4g, this gives a direct view of the most common orientations of the surface magnetization, i.e. the magnetic surface easy axes.

The orientation of magnetic domains on the (001) surface determined by SPLEEM are shown in Fig. 5, for three temperatures: room temperature in panel (a), a temperature below the isotropic point but above the Verwey transition in panel (b), and a temperature below the Verwey transition in panel (c). In the first case, the domains present wavy domain walls.

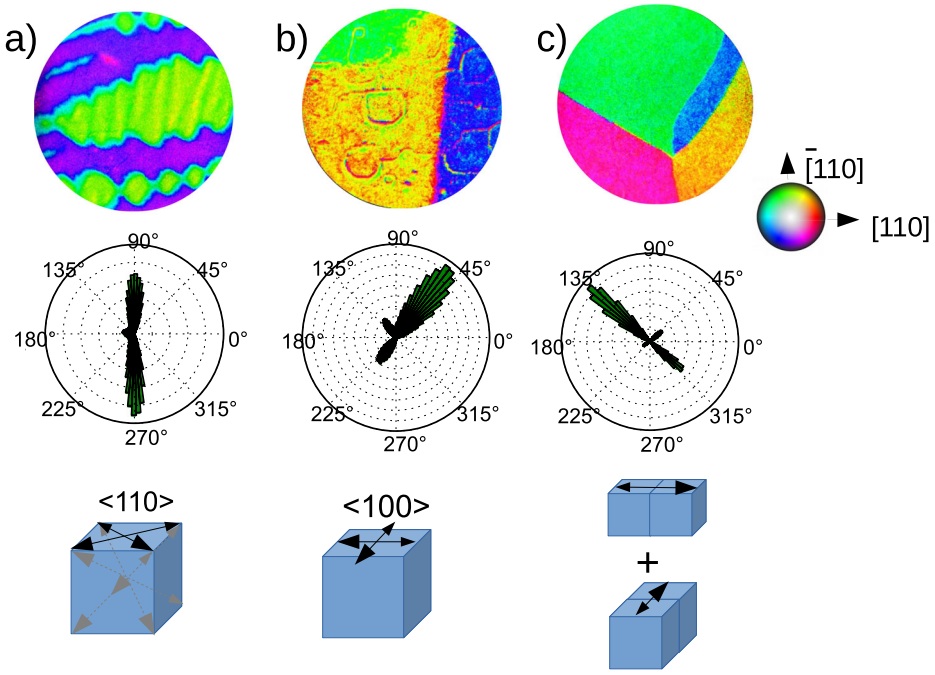

Fig. 5 Magnetization direction as a function of temperature on the (001) surface of magnetite. On each column, a combined SPLEEM color image represents the magnetization according to the map shown on the right side, which also indicates the crystal directions. In the middle, an histogram of the magnetization directions are shown. In the bottom, an schematic indicates the presumed origin of the magnetization directions relative to the cubic spinel unit cell. **a** Room temperature. **b** 137 K, **c** 100 K. Adapted from Refs. [35, 36]

The orientation of the magnetization in the different domains is mostly along the in-plane ⟨110⟩ directions (note that the sample is oriented so the crystallographic [110] direction is along the x-axis. The expected bulk magnetization directions are the ⟨111⟩ family. However, the shape anisotropy brings the magnetization into the surface plane to minimize the stray field. Thus, instead of the ⟨111⟩ magnetization directions, the observed ones correspond to the projection of those directions onto the (001) plane, i.e. the in-plane ⟨110⟩ ones [34, 35].

Upon crossing the isotropic point, the first order magnetocrystalline anisotropy changes its sign, and the easy axes switch to the [100] and [010] directions [4]. Those easy axes are contained within the surface plane, so there is no competition with the shape anisotropy in this case. The magnetization is then oriented along the diagonals in Fig. 5b.

Finally, cooling below the Verwey transition, the cubic crystal transforms into a monoclinic polycrystal [10, 36], where areas that share the same average monoclinic c-axes present the microtwins shown in Fig. 3. But different regions of the crystal have the monoclinic c-axis oriented along different formerly equivalente cubic (001) directions. In each region with the same averaged c-axis, the magnetization is along such axis, as monoclinic sub-Verwey magnetite has a uniaxial magnetocrystalline anisotropy. These magnetic domains are observed to be along the local c-axis, with two orientations (green and purple areas of Fig. 5c, which share a common average c-axis, and blue-yellow areas, which share another c-axis).

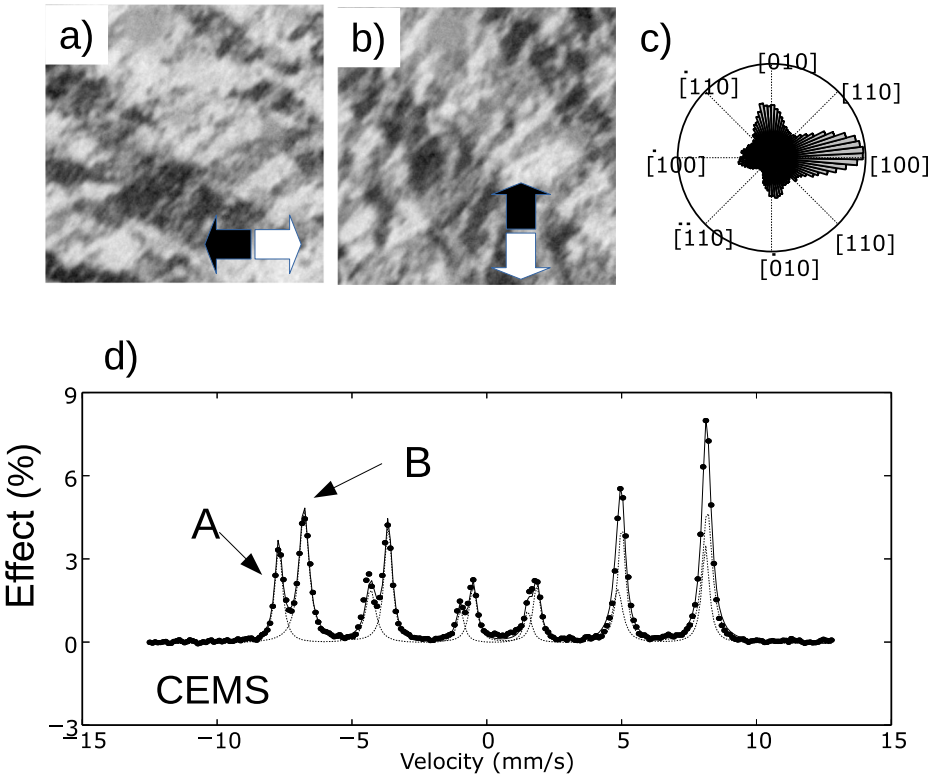

Fig. 6 **a**, **b** Magnetic contrast on the surface of the film observed with SPLEEM. The images are 9.1 μm wide, and are acquired at an electron energy of 6.8 eV. **c** Polar plot of the magnetization. **d** Conversion Electron Mössbauer spectrum from a magnetite single crystal at room temperature. Adapted from Ref. [37]

Note that this is only true for the (001) surface of bulk single crystals. Given the interest of using magnetite in spintronic applications, it is relevant to check whether the observed magnetization directions are also valid for thin films. Thin films, even single crystal ones, can be subject to strains or other defects that change their magnetic properties. In Fig. 6 data acquired on a magnetite film grown on a Nb-doped $SrTiO_3$(001) substrate [37] is shown. The film has been grown by pulsed laser deposition, and characterized by several techniques, among them SPLEEM. The SPLEEM images have been used to determine the magnetic easy axes of the film (Fig. 6a–b). As shown more directly in the magnetization histogram plot of Fig. 6c, the easy axes are along the in-plane [100] and [010] directions. Now, SPLEEM is rather surface sensitive, probing a sub-nanometer depth [25]. In order to check whether the magnetization directions within the film also follow the observed surface direction (something that it is known not to happen for bulk samples at micrometer depths [35]), the magnetization easy axes were also determined by magneto-optic Kerr effect, which samples the full thickness of the 160 nm thick film. The same in-plane [100] and [010] axes were detected.

In Fig. 6d, the conversion electron Mössbauer spectrum (CEMS) for the same sample is presented, with the gamma-ray beam perpendicular to the sample. The room temperature Mössbauer spectra shows the two Zeeman sextets discussed for bulk magnetite. The

Mössbauer parameters, and the relative areas of both are in good agreement with the assignment of each sextet to Fe^{3+} in tetrahedral sites, and $Fe^{2.5+}$ in octehedral sites respectively [37]. Note that, as for bulk samples, the octahedral sextet is broader than the tetrahedral one. We note that while the shift due to the relative orientation of the magnetic axis and the electric field gradient direction will be affected, the dipolar interaction that gives rise to different local magnetic fields still applies. Thus, the explanation put forward for bulk samples [16] applies for the thin film, even if the easy axis are *not* along the ⟨111⟩ directions, but instead the [100] and the [010] directions.

Another interesting detail is that the ratio of the peaks of each sextet are close to 3:2:1. This implies, given the measuring geometry, the presence of an fraction of domains with a magnetization component out-of-plane. Similar observations have been reported by several groups [38–40]. However such magnetization has not been observed by SPLEEM nor by Kerr-effect. The discrepancy with SPLEEM could be ascribed to the surface sensitivity of the latter technique, arguing that the out-of-plane domains are deeper in the film, or even at the substrate-film interface. However a different explanation has to be invoked to explain the lack of out-of-plane magnetization in the Kerr measurements [37]. Instead, in this case, it can be argued that the out-of-plane domains present a much higher coercivity outside the range explored by the Kerr experiment [40]. The origin of such anomalous magnetic properties is linked to the presence of antiphase domain boundaries, boundaries that have been since characterized in detail in magnetite films and that arise from the coalescence of the nuclei that give rise to a complete magnetite film [40–42]. These antiphase boundaries have also been held responsible for superparamagnetism in ultra-thin magnetite films [43], while magnetite structures lacking them show magnetic order at the nanometer limit [44].

5 Mössbauer observations of surfaces and ultra-thin films of magnetite

Mössbauer spectra, either in CEMS [45] or in integral low-energy electron mode [46, 47], should be able to provide additional information on the subject of the role of surfaces and the possible effect of confined geometries such as thin films in the Verwey transition. For example, it is known that for ultrathin films the metal-insulator transition is reduced for small thicknesses, and even disappears for nanoparticles below 10 nm in size [48].

Variable temperature CEMS, from room temperature to 100 K, has been used by Korecki et al. [49–52] on films grown on MgO and Pt. For films grown on MgO(001), they have determined that films thinner than 10 nm do not present a Verwey transition [49]. In Fig. 7 the Mössbauer spectra for the 20 nm film below the Verwey transition is shown, together with the spectra for a 400 nm film in the inset. Korecki et al. determined that the reconstructed surface is richer in Fe^{3+}, as proposed for the reconstructed surface model [14]. However, the interaction of the reconstructed surface with the bulk trimeron model is still under study. Furthermore, understanding the high temperature surface reconstruction transition or to glean further details on the interaction of the Verwey transition with surfaces in thin films and surfaces awaits new experiments. We note in this area the scarcity of instruments available in the world for such studies, with only one in regular use [52].

We finally mention one venue that might provide a path to obtain spatially resolved Mössbauer information with surface sensitivity. A low-energy electron microscope, as described in the previous paragraphs, allows to image electrons emitted from the surface. In LEEM, electrons from an electron gun are used to form an image after being elastically scattered by the sample. In photoemission electron microscopy (PEEM, [53]), the same instrument can be used to form an image with electrons arising from x-ray absorption, a

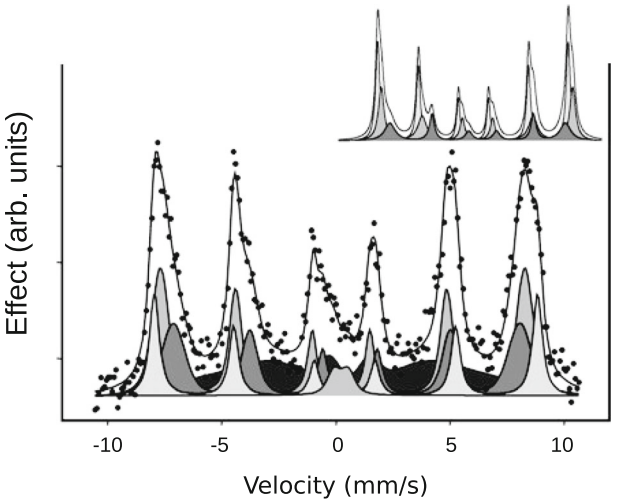

Fig. 7 Conversion electron Mössbauer spectrum of a (001)-oriented magnetite film on MgO(001). The film thickness is 20 nm thick, and the measurement temperature is 85 K. The inset shows the spectrum for a 400 nm thick layer. Adapted with permission from Ref. [50]

technique often applied to magnetite surfaces [54, 55] and films [44]. The same instrument might be used to image conversion electrons emitted after recoiless nuclear resonant absorption. To get a reasonable flux of such electrons would require the use of synchrotron sources [56]. Since in practice PEEM instruments are only used at synchrotrons for x-ray absorption experiments, this would not appear to be a problematic requirement.

6 Summary

Magnetite in general, and the Verwey transition in particular has been studied by Mössbauer spectroscopy since the discovery of the technique. The recent determination of the atomic structure of the low-temperature monoclinic phase has helped to understand the Mössbauer spectrum of magnetite. However, the role of surfaces on the Verwey transition as well as dimensionality effects in thin magnetite films remain much less explored. The technique is capable of providing relevant information in this ongoing quest to understand the oldest metal insulator transition known to the scientific community. In the future we hope that the combination of low-energy electron microscopy and Mössbauer spectroscopy with synchrotron sources might provide a spatially resolved and surface sensitive Mössbauer technique.

Acknowledgements This research was partially supported by the Spanish Ministry of Economy and Competitiveness No. MAT2015-64110-C2-1-P, the Comunidad Autónoma de Madrid NANOMAGCOST-CM project with Ref. P2018/NMT-4321, the European Commission through Project H2020 No. 720853 (Amphibian) and the Chilean FONDECYT Project No. 1161117.

References

1. Mills, A.A.: The lodestone: history, physics, and formation. Ann. Sci. **61**, 273 (2004)
2. Bragg, W.H.: The structure of magnetite and the spinels. Nature **95**, 561 (1915)

3. Cornell, R.M., Schwertmann, U.: The Iron Oxides. Wiley, New York (1997)
4. Aragón, R.: Cubic magnetic anisotropy of nonstoichiometric magnetite. Phys. Rev. B **46**, 5334–5338 (1992)
5. Muxworthy, A.R., McClelland, E.: Review of the low-temperature magnetic properties of magnetite from a rock magnetic perspective. Geophys. J. Int. **140**, 101–114 (2000)
6. Verwey, E.J.W.: Electronic conduction of magnetite Fe_3O_4 and its transition point at low temperatures. Nature **144**, 327–328 (1939)
7. Walz, F.: The Verwey transition - a topical review. J. Phys. Cond. Mat. **14**, R285–R340 (2002)
8. García, J., Subías, G.: The Verwey transition-a new perspective. J. Phys. Cond. Mat. **16**, R145–R178 (2004)
9. Kasama, T., Church, N.S., Feinberg, J.M., Dunin-Borkowski, R.E., Harrison, R.J.: Direct observation of ferrimagnetic/ferroelastic domain interactions in magnetite below the Verwey transition. Earth Plan. Sci. Lett. **297**, 10–17 (2010)
10. de la Figuera, J., Novotny, Z., Setvin, M., Liu, T., Mao, Z., Chen, G., N'Diaye, A.T., Schmid, M., Diebold, U., Schmid, A.K., Parkinson, G.S.: Real-space imaging of the Verwey transition at the (100) surface of magnetite. Phys. Rev. B **88**, 161410 (2013)
11. Senn, M.S., Wright, J.P., Attfield, J.P.: Charge order and three-site distortions in the Verwey structure of magnetite. Nature **481**, 173–176 (2012)
12. Parkinson, G.S.: Iron oxide surfaces. Surf. Sci. Rep. **71**, 272–365 (2016)
13. Lodziana, Z.: Surface Verwey transition in magnetite. Phys. Rev. Lett. **99**, 206402 (2007)
14. Bliem, R., McDermott, E., Ferstl, P., Setvin, M., Gamba, O., Pavelec, J., Schneider, M.A., Schmid, M., Diebold, U., Blaha, P., Hammer, L., Parkinson, G.S.: Subsurface cation vacancy stabilization of the magnetite (001) surface. Science **346**, 1215–1218 (2014)
15. Bauminger, R., Cohen, S.G., Marinov, A., Ofer, S., Segal, E.: Study of the low-temperature transition in magnetite and the internal fields acting on iron nuclei in some spinel ferrites, using Mössbauer absorption. Phys. Rev. **122**, 1447–1450 (1961)
16. Häggström, L., Annersten, H., Ericsson, T., Wäppling, R., Karner, W., Bjarman, S.: Magnetic dipolar and electric quadrupolar effects on the Mössbauer spectra of magnetite above the Verwey transition. Hyperfine Interact. **5**, 201 (1977)
17. Chlan, V., Żukrowski, J., Bosak, A., Kakol, Z., Kozłowski, A., Tarnawski, Z., Řezníček, R., Štěpánková, H., Novák, P., Biało, I., Honig, J.M.: Effect of low Zn doping on the Verwey transition in magnetite single crystals: Mössbauer spectroscopy and x-ray diffraction. Phys. Rev. B **98**, 125138 (2018)
18. Vandenberghe, R.E., De Grave, E.: Mössbauer effect studies of oxidic spinels. In: Long, G.J., Grandjean, F. (eds.) Mössbauer Spectroscopy Applied to Inorganic Chemistry. Modern Inorganic Chemistry, pp. 59–182. Springer, US (1989)
19. Berry, F.J., Skinner, S., Thomas, M.F.: Mössbauer spectroscopic examination of a single crystal of Fe_3O_4. J. Phys.: Cond. Matt. **10**, 215–220 (1998)
20. Řezníček, R., Chlan, V., Štěpánková, H., Novák, P., Żukrowski, J., Kozłowski, A., Kakol, Z., Tarnawski, Z., Honig, J.M.: Understanding the Mössbauer spectrum of magnetite below the Verwey transition: ab initio calculations, simulation, and experiment. Phys. Rev. B **96**, 195124 (2017)
21. Řezníček, R., Chlan, V., Štěpánková, H., Novák, P.: Hyperfine field and electronic structure of magnetite below the Verwey transition. Phys. Rev. B **91**, 125134 (2015)
22. Sawatzky, G.A., Coey, J.M.D., Morrish, A.H.: Mössbauer study of electron hopping in the octahedral sites of Fe_3O_4. J. Appl. Phys. **40**, 1402–1403 (1969)
23. Stanka, B., Hebenstreit, W., Diebold, U., Chambers, S.A.: Surface reconstruction of $Fe_3O_4(001)$. Surf. Sci. **448**, 49–63 (2000)
24. McCarty, K.F., de la Figuera, J.: Low-energy electron microscopy. In: Surface Science Techniques. Springer Series in Surface Sciences, vol. 51, p. 531. Springer, Berlin (2013)
25. Bauer, E.: Surface Microscopy with Low Energy Electrons. Springer, Berlin (2014)
26. de la Figuera, J., Puerta, J.M., Cerda, J.I., El Gabaly, F., McCarty, K.F.: Determining the structure of Ru(0001) from low-energy electron diffraction of a single terrace. Surf. Sci. **600**, L105–L109 (2006)
27. Pentcheva, R., Wendler, F., Meyerheim, H.L., Moritz, W., Jedrecy, N., Scheffler, M.: Jahn-Teller stabilization of a "Polar" metal oxide surface: $Fe_3O_4(001)$. Phys. Rev. Lett. **94**, 126101 (2005)
28. Pentcheva, R., Moritz, W., Rundgren, J., Frank, S., Schrupp, D., Scheffler, M.: A combined DFT/LEED-approach for complex oxide surface structure determination: $Fe_3O_4(001)$. Surf. Sci. **602**, 1299–1305 (2008)
29. Bartelt, N.C., Nie, S., Starodub, E., Bernal-Villamil, I., Gallego, S., Vergara, L., McCarty, K.F., de la Figuera, J.: Order-disorder phase transition on the (100) surface of magnetite. Phys. Rev. B **88**, 235436 (2013)

30. Novotný, Z., Argentero, G., Wang, Z., Schmid, M., Diebold, U., Parkinson, G.S.: Ordered array of single adatoms with remarkable thermal stability: Au/Fe_3O_4(001). Phys. Rev. Lett. **108**, 216103 (2012)
31. Lindquist, A.K., Feinberg, J.M., Harrison, R.J., Loudon, J.C., Newell, A.J.: The effects of dislocations on crystallographic twins and domain wall motion in magnetite at the Verwey transition. Earth, Planets and Space **71**, 5 (2019)
32. Rougemaille, N., Schmid, A.K.: Magnetic imaging with spin-polarized low-energy electron microscopy. Eur. Phys. J. App. Phys. **50**, 20101 (2010)
33. Duden, T., Bauer, E.: A compact electron-spin-polarization manipulator. Rev. Sci. Inst. **66**, 2861 (1995)
34. de la Figuera, J., Vergara, L., N'Diaye, A., Quesada, A., Schmid, A.: Micromagnetism in (001) magnetite by spin-polarized low-energy electron microscopy. Ultramicroscopy **130**, 77–81 (2013)
35. Martín-García, L., Chen, G., Montana, Y., Mascaraque, A., Pabon, B.M., Schmid, A.K., de la Figuera, J.: Memory effect and magnetocrystalline anisotropy impact on the surface magnetic domains of magnetite(001). Sci. Rep. **8**, 5991 (2018)
36. Martín-García, L., Mascaraque, A., Pabón, B.M., Bliem, R., Parkinson, G.S., Chen, G., Schmid, A.K., de la Figuera, J.: Spin reorientation transition of magnetite (001). Phys. Rev. B **93**, 134419 (2016)
37. Monti, M., Sanz, M., Oujja, M., Rebollar, E., Castillejo, M., Pedrosa, F.J., Bollero, A., Camarero, J., Cuñado, J.L.F., Nemes, N.M., Mompean, F.J., Garcia-Hernández, M., Nie, S., McCarty, K.F., N'Diaye, A.T., Chen, G., Schmid, A.K., Marco, J.F., de la Figuera, J.: Room temperature in-plane ⟨100⟩ magnetic easy axis for Fe_3O_4/$SrTiO_3$(001):Nb grown by infrared pulsed laser deposition. J. Appl. Phys. **114**, 223902 (2013)
38. Margulies, D.T., Parker, F.T., Spada, F.E., Goldman, R.S., Li, J., Sinclair, R., Berkowitz, A.E.: Phys. Rev. B **53**(14), 9175 (1996)
39. Voogt, F.C., Fujii, T., Smulders, P.J.M., Niesen, L., James, M.A., Hibma, T.: NO2-assisted molecular-beam epitaxy of Fe_3O_4, $Fe_{3-\delta}O_4$, and γ-Fe_2O_3 thin films on MgO(100). Phys. Rev. B **60**, 11193 (1999)
40. Kalev, L.A., Niesen, L.: Nuclear resonance scattering study on the spin orientation in an epitaxial layer of Fe_3O_4 on MgO(100). Phys. Rev. B **67**(22), 224403 (2003)
41. Margulies, D.T., Parker, F.T., Rudee, M.L., Spada, F.E., Chapman, J.N., Aitchison, P.R., Berkowitz, A.E.: Origin of the anomalous magnetic behavior in single crystal Fe_3O_4 films. Phys. Rev. Lett. **79**, 5162 (1997)
42. Eerenstein, W.: Spin-dependent transport across anti-phase boundaries in magnetite films. Ph.D. Thesis, Rijskuniversisteit, Groningen (2003)
43. Voogt, F.C., Palstra, T.T.M., Niesen, L., Rogojanu, O.C., James, M.A., Hibma, T.: Phys. Rev. B **57**, R8107 (1998)
44. Monti, M., Santos, B., Mascaraque, A., Rodríguez de la Fuente, O., Niño, M.A., Mentes, T.O., Locatelli, A., McCarty, K.F., Marco, J.F., de la Figuera, J.: Magnetism in nanometer-thick magnetite. Phys. Rev. B **85**, 020404 (2012)
45. Gancedo, J.R., Gracia, M., Marco, J.F.: CEMS methodology. Hyperfine Interact. **66**, 83–93 (1991)
46. De Grave, E., Vandenberghe, R.E., Dauwe, C.: ILEEMS: methodology and applications to iron oxides. Hyperfine Interact. **161**, 147–160 (2005)
47. Marco, J.F., Gancedo, J.R., Monti, M., de la Figuera, J.: Mössbauer spectroscopy and surface analysis. In: Mössbauer Spectroscopy, pp. 455–469. Wiley (2013)
48. Lee, J., Kwon, S.G., Park, J.-G., Hyeon, T.: Size dependence of metal-insulator transition in stoichiometric Fe_3O_4 nanocrystals. Nano Lett. **15**, 4337–4342 (2015)
49. Korecki, J., Handke, B., Spiridis, N., Slezak, T., Flis-Kabulska, I., Haber, J.: Size effects in epitaxial films of magnetite. Thin Solid Films **412**, 14–23 (2002)
50. Spiridis, N., Handke, B., Slezak, T., Barbasz, J., Zajac, M., Haber, J., Korecki, J.: Surface structure of epitaxial magnetite Fe_3O_4(001) films: in situ STM and CEMS studies. J. Phys. Chem. B **108**, 14356–14361 (2004)
51. Kim-Ngan, N.T.H., Balogh, A.G., Meyer, J.D., Brotz, J., Hummelt, S., Zajac, M., Slezak, T., Korecki, J.: Structure, composition and crystallinity of epitaxial magnetite thin films. Surf. Sci. **602**, 2358–2362 (2008)
52. Spiridis, N., Wilgocka-Slezak, D., Freindl, K., Figarska, B., Giela, T., Mlynczak, E., Strzelczyk, B., Zajac, M., Korecki, J.: Growth and electronic and magnetic structure of iron oxide films on Pt(111). Phys. Rev. B **85**, 075436 (2012)
53. Schneider, C.M., Schönhense, G.: Investigating surface magnetism by means of photoexcitation electron emission microscopy. Rep. Prog. Phys. **65**, 1785–1839 (2002)
54. Martín-García, L., Gargallo-Caballero, R., Monti, M., Foerster, M., Marco, J.F., Aballe, L., de la Figuera, J.: Spin and orbital magnetic moment of reconstructed $\sqrt{2} \times \sqrt{2}$R45° magnetite(001). Phys. Rev. B **91**, 020408 (2015)

55. Gargallo-Caballero, R., Martín-García, L., Quesada, A., Granados-Miralles, C., Foerster, M., Aballe, L., Bliem, R., Parkinson, G.S., Blaha, P., Marco, J.F., de la Figuera, J.: Co on Fe_3O_4(001): towards precise control of surface properties. J. Chem. Phys. **144**, 094704 (2016)
56. Potapkin, V., Chumakov, A.I., Smirnov, G.V., Celse, J.-P., Rüffer, R., McCammon, C., Dubrovinsky, L.: The ^{57}Fe synchrotron Mössbauer source at the ESRF. J. Synchrotron Radiat. **19**, 559–569 (2012)